Journal of ELECTRONIC MATERIALS, Vol. 47, No. 9, 2018
https://doi.org/10.1007/s11664-018-6252-3
© 2018 The Minerals, Metals & Materials Society

TOPICAL COLLECTION: 17TH CONFERENCE ON DEFECTS (DRIP XVII)

Observation of Threading Dislocations in Ammonothermal Gallium Nitride Single Crystal Using Synchrotron X-ray Topography

Y. YAO,[1,3] Y. ISHIKAWA,[1] Y. SUGAWARA,[1] Y. TAKAHASHI,[2] and K. HIRANO[2]

1.—Japan Fine Ceramics Center (JFCC), Nagoya 456-8587, Japan. 2.—High Energy Accelerator Research Organization (KEK), 1-1 Ooho, Tsukuba 305-0801, Japan. 3.—e-mail: y_yao@jfcc.or.jp

Synchrotron monochromatic-beam x-ray topography observation has been performed on high-quality ammonothermal gallium nitride single crystal to evaluate threading dislocations (TD) in a nondestructive manner. Asymmetric diffractions with six equivalent $\boldsymbol{g}$-vectors of 11–26, in addition to a symmetric diffraction with $\boldsymbol{g}$ = 0008, were applied to determine the Burgers vectors ($\boldsymbol{b}$) of dislocations. It was found that pure edge-type TDs with $\boldsymbol{b} = \langle 11-20 \rangle /3$ did not exist in the sample. A dominant proportion of TDs were of mixed type with $\boldsymbol{b} = \langle 11-20 \rangle /3 + \langle 0001 \rangle$, i.e., so-called $c + a$ dislocations. Pure 1c screw dislocations with $\boldsymbol{b} = \langle 0001 \rangle$ and TDs with c-component larger than 1c were also observed.

Key words: GaN, ammonothermal, dislocation, synchrotron x-ray topography, Burgers vector

INTRODUCTION

In recent years, gallium nitride (wz-GaN) has attracted increasing attention as one of the most promising wide-bandgap semiconductor materials for next-generation power electronic devices.[1,2] To improve device reliability under high power density and high operating temperature, GaN substrate and epitaxial layer with dislocations below 10^4 cm^{-2} to 10^5 cm^{-2} are desirable, which is about two orders of magnitude lower than the typical level at present.[3–5] Recently, it was reported that GaN single crystals with dislocation density around 10^4 cm^{-2} can be achieved by ammonothermal method.[6–9]

Evaluating dislocations in GaN in a nondestructive manner is of great importance, as it enables further crystal growth and device fabrication afterwards. In particular, techniques that can reveal the dislocation distribution across large sample area and dislocation types with high spatial resolution are urgently required for growth condition optimization and device failure analysis. Synchrotron x-ray topography (XRT) is a powerful tool to fulfill these requirements. It has been used extensively to study dislocations in semiconductor materials such as silicon carbide (SiC).[10–13] In this work, we carried out XRT observation on an ammonothermal GaN single crystal to reveal and categorize threading dislocations (TD) according to their Burgers vector ($\boldsymbol{b}$).

EXPERIMENTAL PROCEDURES

A commercially available GaN ($10 \times 10 \times 0.42$ t mm^3, n-type, on-axis) sample was observed. It was grown by ammonothermal method. x-Ray diffraction (XRD) measurements on this sample showed a full-width at half-maximum (FWHM) of (1–105) reflection of about 20 arcsec, and a curvature of radius of {0001} planes greater than 100 m. This large radius of curvature in comparison with typical hydride vapor-phase epitaxy (HVPE) GaN has been found to be an indispensable characteristic for XRT observation. Synchrotron monochromatic-beam XRT (λ = 1.127 Å) was recorded from the chemical–mechanical polishing (CMP)-treated

(Received November 28, 2017; accepted March 21, 2018; published online April 2, 2018)

Ga-face at beamline BL-3C of the Photon Factory at the High-Energy Accelerator Research Organization (KEK), Japan. Asymmetric diffractions with six equivalent diffraction vectors $\boldsymbol{g}$ of 11–26 were applied by rotating the sample every 60° with respect to its surface normal, in addition to a symmetric diffraction with $\boldsymbol{g}$ = 0008. The diffraction planes (visualized by VESTA)[14] used and experimental settings are shown in Fig. 1. X-rays diffracted from the samples were first collected by a PiN diode detector to optimize the sample position. Then, a charge-coupled device (CCD) detector was used to preview the topography image. Finally, nuclear emulsion plates were used to record XRT with high spatial resolution. The topmost 10-μm surface of the sample makes the major contribution to the XRT images.

RESULTS AND DISCUSSION

Dislocations in GaN are mainly TDs propagating nearly along the c-axis. They can be categorized into

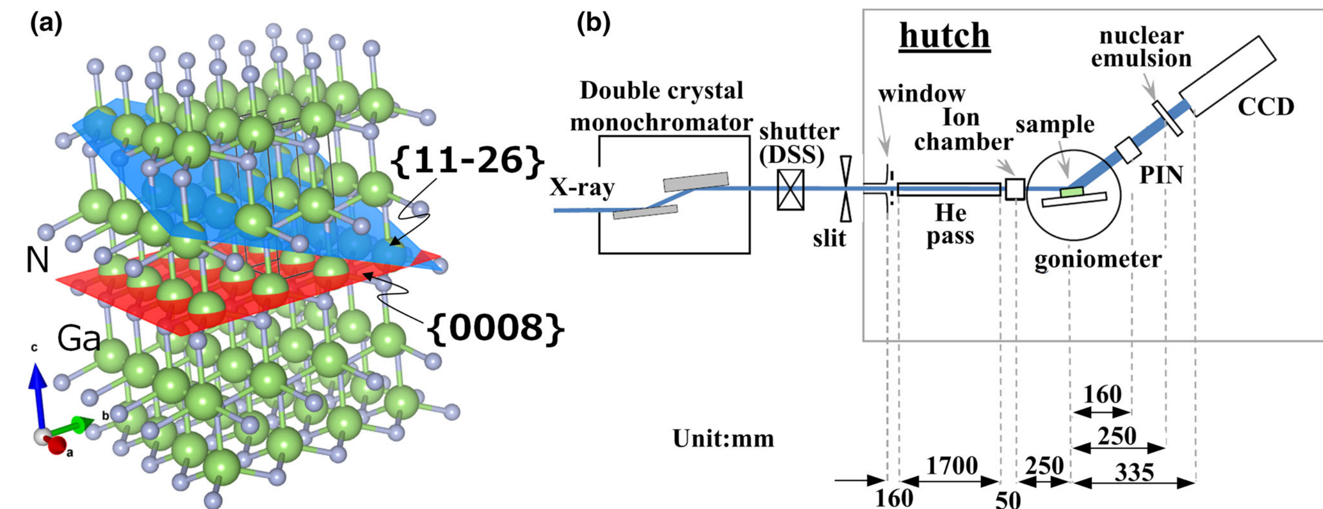

Fig. 1. (a) Crystal structure of wz-GaN and diffraction planes used for XRT observation. (b) Experimental setup for XRT observation.

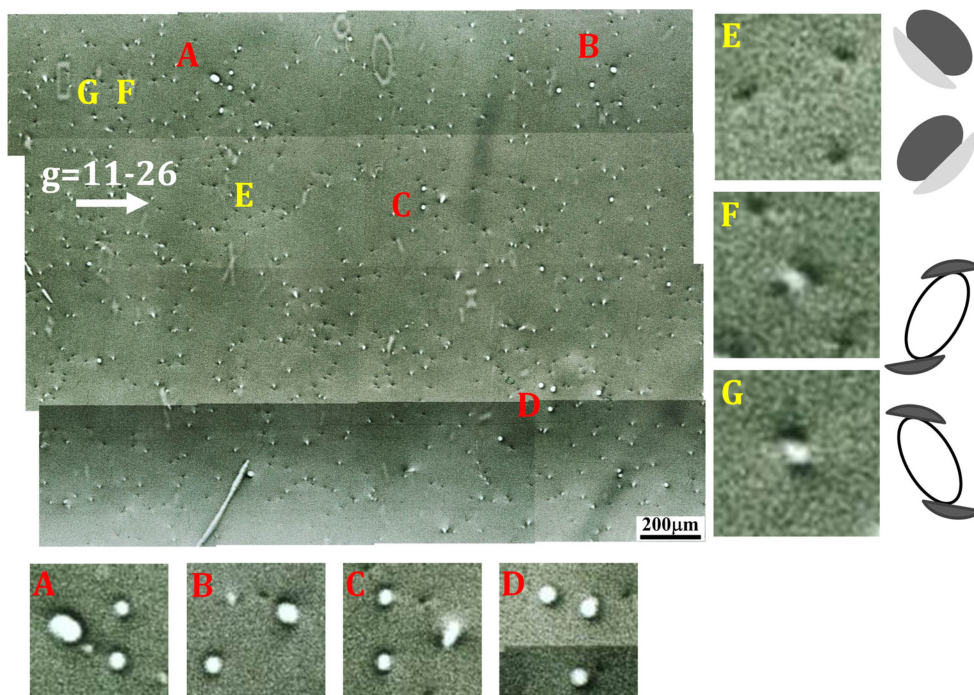

Fig. 2. XRT image of area of 2.3 × 1.8 mm^2 of GaN, taken with diffraction vector $\boldsymbol{g}$ = 11–26. (a)–(d) indicate relatively large spots, while (e)–(g) indicate small spots. Dark shadows are found on a certain side of the spot outlines.

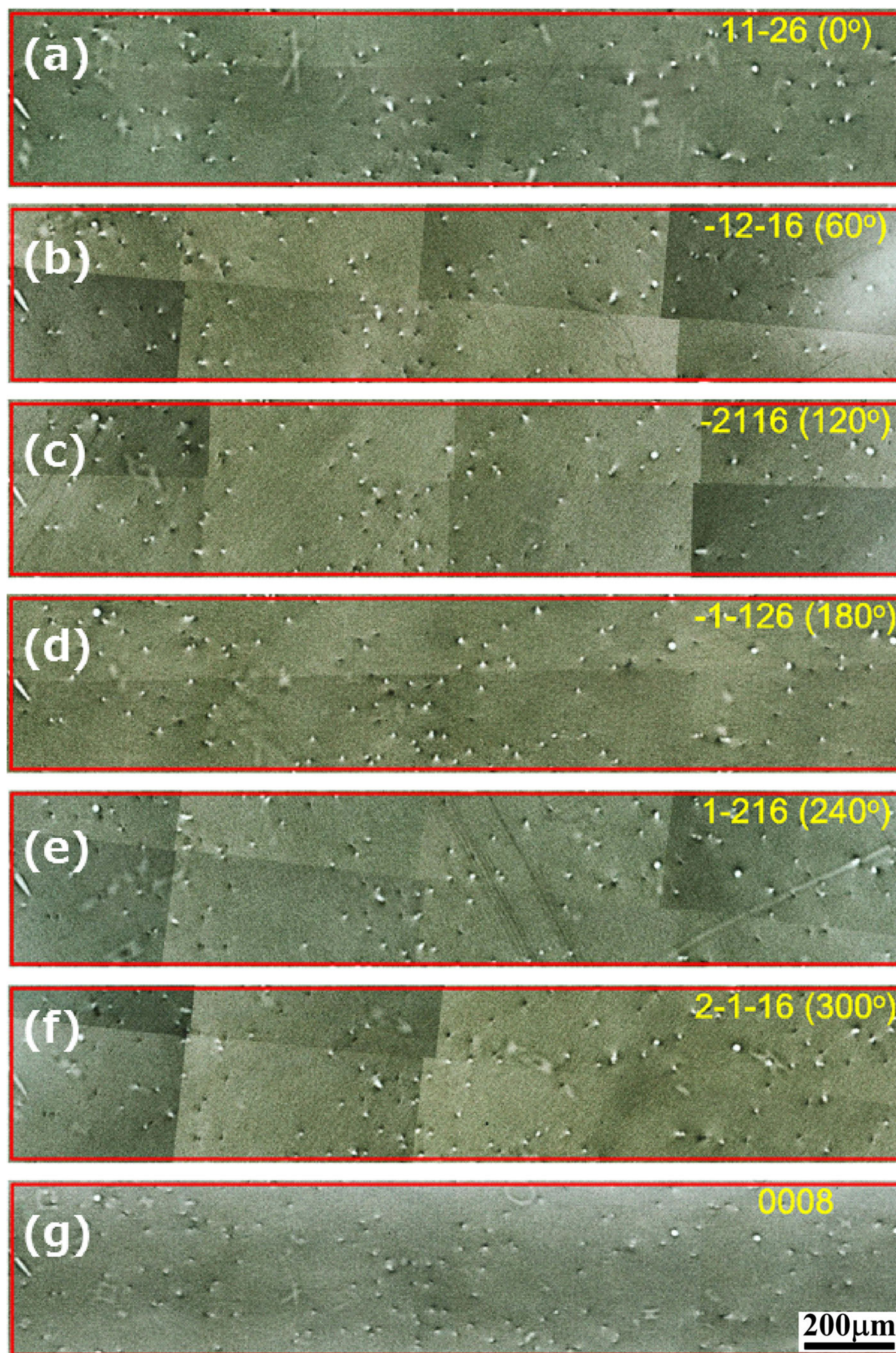

Fig. 3. XRT images taken from the same sample position with (a–f) six equivalent ***g***-vectors of 11–26, and (g) ***g*** = 0008.

edge type (ED, ***b*** = *ma*), screw-type (SD, ***b*** = *nc*), and mixed-type (MD, ***b*** = *nc* + *ma*; *n*, *m* = 1, 2, etc.), according to their Burgers vector. The different types of TDs may have different growth-related origins, and in real device applications they contribute differently to device degradation.

Figure 2 shows the XRT image of an area of $2.3 \times 1.8\ \mathrm{mm}^2$, taken with diffraction vector ***g*** = 11–26. Spot-shaped contrasts in the image are attributed to TDs; no line-shaped contrasts were observed, indicating that the sample surface was nearly free of basal plane dislocations. Judging from the spot size, most of them are relatively small (like the ones marked by E–G), and dark shadows are found on a certain side of the spot outlines, as discussed below. In comparison, some spots were of larger size (like those marked by A–D), being typically of round shape with uniform dark outline.

Figure 3 shows XRT images taken from the same sample position with six equivalent ***g***-vectors of

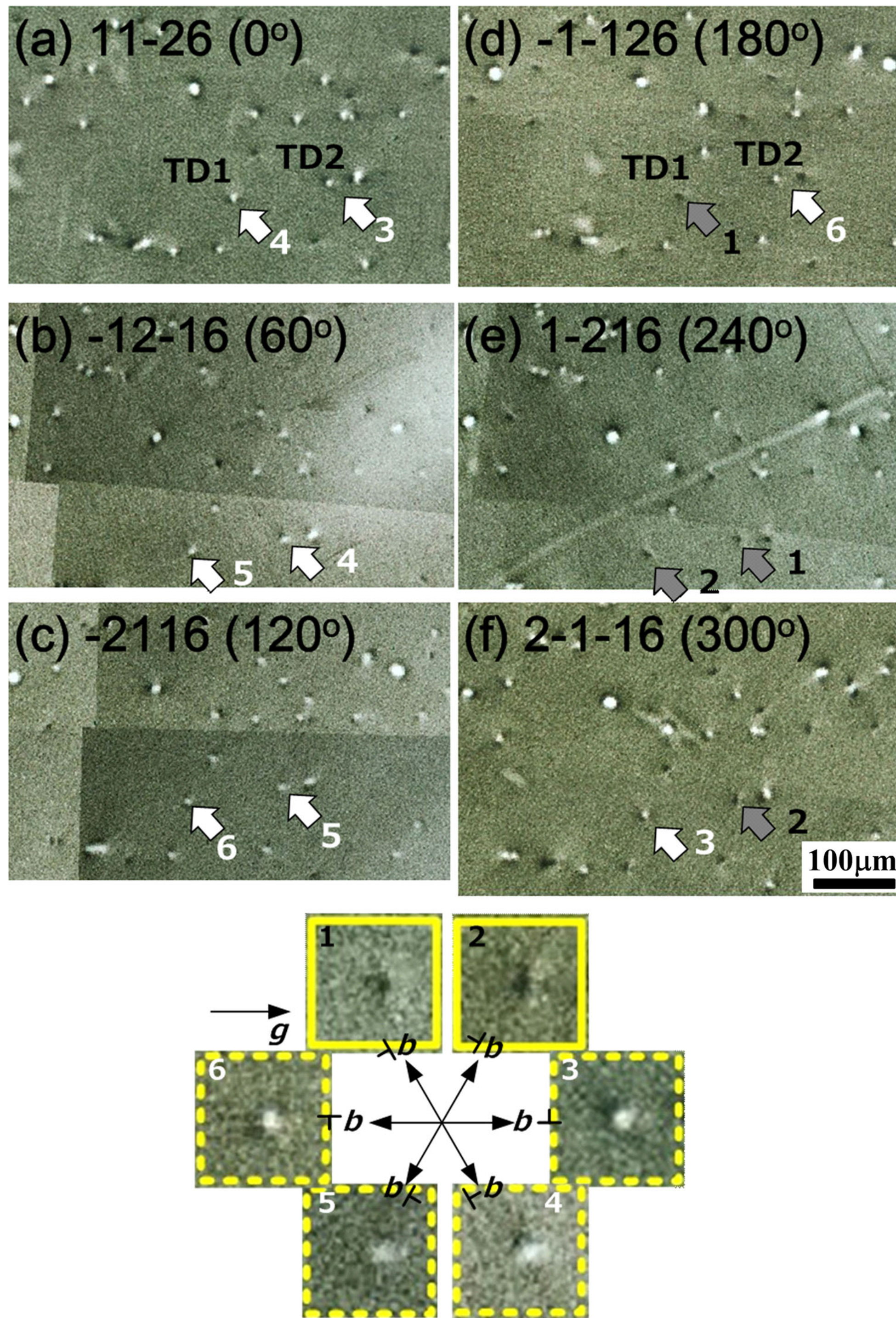

Fig. 4. Changes in dark/bright contrast of $c + a$ TD spots when the $\boldsymbol{g}$-vector is changed among six equivalent 11–26 from (a) to (f).

11–26, and $\boldsymbol{g}$ = 0008. Spot-shaped contrasts in all images show one-to-one correlation in position, although the same spot may appear as bright in some images but dark in others. According to the $\boldsymbol{g}\cdot\boldsymbol{b}$ invisibility criterion, images taken with $\boldsymbol{g}$ = 11–26 should reveal all three types of TDs, while the image with $\boldsymbol{g}$ = 0008 should reveal TDs whose $\boldsymbol{b}$ contains a c-component (SD or MD). It is clear that no pure EDs exist in this sample. According to ray-tracing simulation results on 4H-SiC,[11] which has a similar hexagonal structure to GaN, the spot sizes in an XRT image reflect the magnitude of $\boldsymbol{b}$ of dislocations. Therefore, small spots in Figs. 2 and 3 are attributed to TDs with $\boldsymbol{b} = \langle 0001 \rangle$ (pure 1c SD)

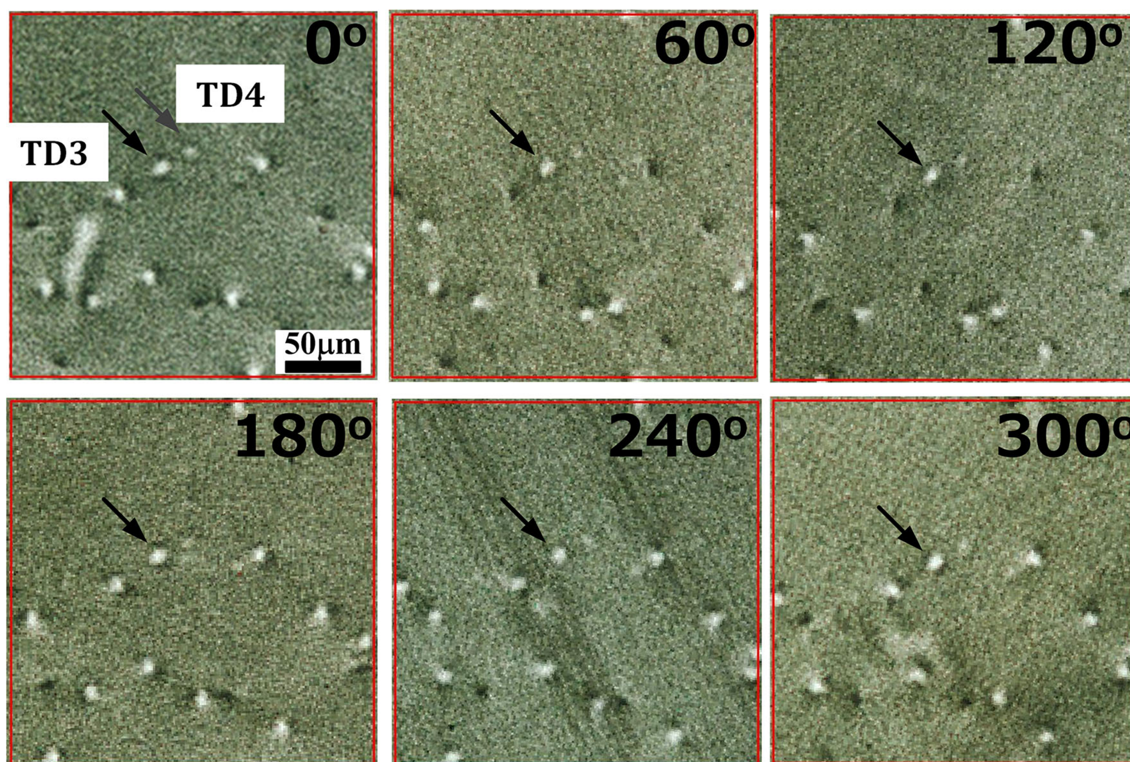

Fig. 5. Pure 1*c* screw-type TD that appears as a bright spot in all six images of 11–26 diffraction.

Table I. TDs with various Burgers vectors and their proportions, obtained from XRT observation

Burgers Vector (*b*)	TD Type	Proportion (%)
1*a*	Edge	0
1*c*	Screw	1
1*c* + 1*a*	Mixed	96
With 2*c* or larger	Screw or mixed	3

or $\boldsymbol{b} = \langle 11\text{–}20\rangle/3 + \langle 0001\rangle$, viz. so-called $c + a$ dislocations, and large spots to TDs with *c*-component of 2*c* or larger.

Figure 4 shows the change in dark/bright contrast of $c + a$ TD spots when the $\boldsymbol{g}$-vector is changed among the six equivalent 11–26 (i.e., changing phi from 0° to 300° in steps of 60°). Using TD1 as an example, it first appears as a dark spot in Fig. 4d and then Fig. 4e, but appears as a bright spot in the other four images. TD2 shows similar results but with 60° difference in phi. Comparing these results with the XRT spot contrast for threading edge dislocations in 4H-SiC,[13] it is clear that these changes in dark or bright contrast (i.e., two dark + four bright) originates from the direction of the *a*-component of $\boldsymbol{b}$ with respect to the $\boldsymbol{g}$-vector. In this way, the direction of the *a*-component of $c + a$ TDs in GaN can be unambiguously determined.

Next, we examined whether there were any pure 1*c* screw-type TDs in this sample. As marked by TD3 in Fig. 5, we found only one pure 1*c* TD among the 107 TDs investigated. This 1*c* TD appears as a bright spot in all six images of 11–26 diffraction, since it contains no *a*-component. TD4 also seems to be a pure 1*c* TD, but because its contrast was blurred except for the 0° image, it was excluded from the statistics.

As for TDs with very large $\boldsymbol{b}$ of $1a + nc$ ($n = 2, 3, 4$, etc.), a relatively small a/nc ratio would make it difficult to judge the direction of the *a*-component by observing the change in dark/bright contrast of the spots. Instead of such dark/bright change, the spot shape would change from round to "squeezed elliptical shape" in two of the six images if an *a*-component is contained, similar to the case of SiC.[12,15] Results regarding mixed-type TDs with large $\boldsymbol{b}$ will be discussed elsewhere.

Finally, the distribution and density of TDs were investigated. The proportions of the various types of TDs, as revealed by XRT, are presented in Table I. The total count of 676 TDs in an area of $2.3 \times 1.8\ \text{mm}^2$ yields a density of $1.6 \times 10^4\ \text{cm}^{-2}$. A dominant proportion of the TDs were of mixed type with $\boldsymbol{b} = 1a + 1c = \langle 11\text{–}20\rangle/3 + \langle 0001\rangle$, viz. so-called $c + a$ dislocations. The proportion of dark $c + a$ TD spots in Fig. 2 is about 42%, larger than the value of 1/3 that one obtains by assuming that

the *a*-component of the MDs are equally distributed among all six possible directions of ⟨11−20⟩. This implies that a certain direction of *a*-component might be favored over others in the current growth process as used for this sample.

CONCLUSIONS

TDs in ammonothermal GaN were studied by synchrotron XRT at six equivalent ***g***-vectors of 11–26 as well as ***g*** = 0008. Burgers vectors can be determined by observing the size and dark/bright contrast change of spots. The results show that 96% of TDs in this sample were of $c + a$ mixed type, while the rest were pure 1*c* (about 1%) or TDs with larger *c*-component (3%). Pure edge-type dislocations did not exist in this sample, but note that this observation might not be universal for all ammonothermal GaN samples. These results demonstrate the usefulness of XRT as a TD categorization technique for GaN, providing a nondestructive way to investigate the role that each type of TD plays in GaN power devices.

ACKNOWLEDGEMENTS

This work was supported by Super Cluster Program of Japan Science and Technology Agency (JST). XRT was performed under the approval of the Photon Factory Program Advisory Committee (Proposal No. 2016G567).

REFERENCES

1. I.C. Kizilyalli, A.P. Edwards, O. Aktas, T. Prunty, and D. Bour, *IEEE Trans. Electron Dev.* 62, 414 (2015).
2. T. Oka, T. Ina, Y. Ueno, and J. Nishii, *Appl. Phys. Express* 8, 054101 (2015).
3. T. Kachi and T. Uesugi, *Sensor Mater.* 25, 219 (2013).
4. K. Yamane, M. Ueno, H. Furuya, N. Okada, and K. Tadatomo, *J. Cryst. Growth* 358, 1 (2012).
5. Y. Yao, Y. Ishikawa, Y. Sugawara, D. Yokoe, M. Sudo, N. Okada, and K. Tadatomo, *Superlattice Microst.* 99, 83 (2016).
6. S. Sintonen, S. Suihkonen, H. Jussila, A. Danilewsky, R. Stankiewicz, T.O. Tuomi, and H. Lipsanen, *Appl. Phys. Express* 7, 091003 (2014).
7. S. Sintonen, S. Suihkonen, H. Jussila, H. Lipsanen, T.O. Tuomi, E. Letts, S. Hoff, and T. Hashimoto, *J. Cryst. Growth* 406, 72 (2014).
8. S. Sintonen, M. Rudziński, S. Suihkonen, H. Jussila, M. Knetzger, E. Meissner, A. Danilewsky, T.O. Tuomi, and H. Lipsanen, *J. Appl. Phys.* 116, 083504 (2014).
9. N.A. Mahadik, S.B. Qadri, and J.A. Freitas Jr, *Cryst. Growth Des.* 15, 291 (2015).
10. M. Dudley, Y. Chen, X.R. Huang, and R. Ma, *Mater. Sci. Forum* 600–603, 261 (2009).
11. Y. Chen, X.R. Huang, G. Dhanaraj, M. Dudley, E.K. Sanchez, and M.F. MacMillan, *Mater. Sci. Forum* 600–603, 297 (2009).
12. F. Wu, M. Dudley, H. Wang, S. Byrappa, S. Sun, B. Raghothamachar, E.K. Sanchez, G. Chung, D. Hansen, S.G. Mueller, and M.J. Loboda, *Mater. Sci. Forum* 740–742, 217 (2013).
13. I. Kamata, M. Nagano, H. Tsuchida, Y. Chen, and M. Dudley, *Mater. Sci. Forum* 600–603, 305 (2009).
14. K. Momma and F. Izumi, *J. Appl. Crystallogr.* 44, 1272 (2011).
15. Y. Yao, Y. Ishikawa, Y. Sugawara, Y. Takahashi, and K. Hirano, *Mater. Sci. Forum* 897, 185 (2017).